Self-trapped holes in $BaTiO_3$

Worawat Traiwattanapong, Anderson Janotti, Naoto Umezawa, Sukit Limpijumnong, Jiraroj T-Thienprasert, and Pakpoom Reunchan

Citation: Journal of Applied Physics **124**, 085703 (2018); doi: 10.1063/1.5036750
View online: https://doi.org/10.1063/1.5036750
View Table of Contents: http://aip.scitation.org/toc/jap/124/8
Published by the American Institute of Physics

Self-trapped holes in $BaTiO_3$

Worawat Traiwattanapong,[1] Anderson Janotti,[2] Naoto Umezawa,[3] Sukit Limpijumnong,[4,5] Jiraroj T-Thienprasert,[1,4] and Pakpoom Reunchan[1,4,a)]

[1]*Department of Physics, Faculty of Science, Kasetsart University, Bangkok 10900, Thailand*
[2]*Department of Materials Science and Engineering, University of Delaware, Delaware 19716, USA*
[3]*CAE Team, Semiconductor R&D Center, Samsung Electronics, Hwaseong-si, Gyeonggi-do 18448, South Korea*
[4]*Thailand Center of Excellence in Physics (ThEP Center), Commission on Higher Education, Bangkok 10400, Thailand*
[5]*School of Physics and NANOTEC-SUT Center of Excellence on Advance Functional Nanomaterials, Suranaree University of Technology, Nakhon Ratchasima 30000, Thailand*

(Received 18 April 2018; accepted 5 August 2018; published online 23 August 2018)

The behavior of holes in the valence band of $BaTiO_3$ is investigated using hybrid density-functional calculations. We find that holes tend to self-trap, localizing on individual O atoms and causing local lattice distortions, forming small hole-polarons. This takes place even in the absence of intrinsic defects or impurities. The self-trapped hole (STH) is more energetically favorable than the delocalized hole in the valence band. The calculated emission peak energy corresponding to the recombination of a conduction band electron with a STH can explain the observed photoluminescence at low temperatures. The stability of the STH, its migration barrier, and the related emission peak are then compared to those of $SrTiO_3$. *Published by AIP Publishing.*
https://doi.org/10.1063/1.5036750

I. INTRODUCTION

Among the perovskite oxides, barium titanate ($BaTiO_3$) has been widely studied, both experimentally and theoretically, as a ferroelectric,[1–3] high-k dielectric[4,5] and a photorefractive material.[6] Owing to these properties, $BaTiO_3$ is a promising material for many technological applications, including multilayer ceramic capacitors,[7,8] gate dielectrics,[9] photocatalyst,[10,11] and holographic storage.[12] In all these applications, intrinsic point defects and impurities are likely to play important roles. Charge localization, in the form of small polarons, near or in the absence of these defects, is expected to significantly impact the electronic and optical properties of this perovskite oxide.

For another perovskite oxide, $SrTiO_3$, it has been recently proposed that the observed room-temperature blue luminescence is associated with the recombination of a small (electron) polaron bound to an oxygen vacancy and a hole in the valence band,[13] while the recombination of a free electron and a self-trapped hole (STH) was predicted to give rise to the observed green luminescence at low temperatures.[13]

For $BaTiO_3$, it has been reported that the photoconductivity does not scale linearly with light intensity,[14,15] and this effect is often attributed to the presence of hole traps above the valence band, which reduces the lifetime of the free holes.[16,17] The existence of small polarons in $BaTiO_3$ and their effect on the optical and transport properties have long been inferred from experiments and suggested as the cause of green luminescence in single crystals.[18–20] The charge transport properties, such as drift mobility, were explained by small-polaron hopping mechanisms.[21] However, it is currently unclear whether the electron or hole small polarons are the causes of the observed phenomena.

Despite a number of experimental reports focusing on polaronic effects in $BaTiO_3$, only a few theoretical studies are available. A computational modeling study using the embedded molecular cluster model suggested that holes in cubic $BaTiO_3$ are self-trapped instead of being delocalized in the valence band.[22] The polaron absorption energy was also reported and claimed to agree with the experimental observation.[22] Later on, an explanation, based on semi-empirical quantum chemistry modeling, was put forth to explain the observed green luminescence.[23] Recently, improved calculations for the behavior of holes in oxides, based on the hybrid-functional density-functional theory (DFT), were introduced and applied to various metal oxides,[24–27] including the perovskite $SrTiO_3$.[13,28] It was found that a hole in $SrTiO_3$ tends to be self-trapped, localizing on one oxygen atom. The self-trapped hole was proposed to be responsible for the green luminescence in $SrTiO_3$ at low temperatures. However, for the holes in $BaTiO_3$, such a detailed study is not available.

Using hybrid-functional calculations, we investigate the behavior of holes in $BaTiO_3$ and draw comparisons to $SrTiO_3$. Our approach overcomes the shortcoming of the semi-empirical quantum chemistry methods based on Hartree-Fock (HF) formalism that overestimates the bandgap, as well as the local density approximation (LDA) or generalized gradient approximation (GGA) that underestimates the bandgap. Total energies, electronic structures, and structural relaxations are consistently computed within the same framework.

Our results reveal that a hole prefers self-trapping to delocalizing in $BaTiO_3$. The self-trapped hole is even more stable in $BaTiO_3$ than in $SrTiO_3$ and likely to be observed at relatively higher temperatures. The emission peak energy from the recombination of an electron in the conduction band and a self-trapped hole was determined by constructing

a)Author to whom correspondence should be addressed: pakpoom.r@ku.ac.th.

a configuration coordinate diagram and found to give rise to the luminescence at 2.17 eV. Finally, we determined the migration of the self-trapped hole and drew comparisons with available experimental data on the transport properties.

II. METHODOLOGY

Our calculations are based on DFT and the screened hybrid-functional proposed by Heyd, Scuseria, and Ernzerhof (HSE06)[29] as implemented in the VASP code.[30] Projector augmented wave potentials with 10, 4, and 6 valence electrons for Ba ($5s^2 5p^6 6s^2$), Ti ($4s^2 3d^2$), and O ($2s^2 2p^4$) were used to describe interactions between the valence electrons and ionic cores. The use of the standard mixing parameter of 25% HF exchange ($\alpha = 0.25$) gives an indirect bandgap R-Γ of 2.94 eV and a direct gap Γ-Γ of 2.99 eV. The calculated bandgap is slightly smaller than the experimental value of 3.20 eV for the cubic phase.[31] The calculated lattice parameter of 3.994 Å is in excellent agreement with the experimental value of 3.996 Å.[32] Compared to other theoretical approaches that are generally employed to correct the wave-function localization of defects such as HF,[33] DFT+U,[26,34] or self-interaction correction,[35] HSE06 functional has been proven to be a useful tool to accurately describe the electronic structure of host materials and defect levels. The standard mixing parameter of the HF exchange ($\alpha = 0.25$) was suggested to correctly describe polaronic and defect levels in group-IV semiconductors[36] and TiO_2[37] as the self-interaction error is minimized, and thereby, the generalized Koopmans theorem is fulfilled. Often, optimizing HF mixing parameters to best reproducing the experimental bandgap is done for polarons and defects calculations of metal oxides. However, the conclusions are generally not very sensitive to the choice of α.[24,38] Recently, optimized HSE was demonstrated to successfully reproduce the bandgap and predict the accurate defect level in Ga_2O_3.[39] Test calculations show that the self-interaction error is small for $\alpha = 0.25$, and our qualitative conclusion remains valid for $\alpha = 0.30$, which reproduces the experimental bandgap (see supplementary material).

To study a small polaron, a supercell of 135 atoms, which is a $3 \times 3 \times 3$ repetition of the five-atom primitive cell of cubic $BaTiO_3$, is used as the starting structure. A single special k-point (1/4, 1/4, 1/4), which is equivalent to 27 k-points in a primitive cell, was used for integrations over the Brillouin zone of the supercell, and the energy cutoff for the plane-wave expansion was set to 400 eV. All atoms were relaxed until the residual forces are less than 0.01 eV/Å. Similar settings were adopted to calculate the hole localization in the cubic $SrTiO_3$ for comparison. Note that while we choose to study both $SrTiO_3$ and $BaTiO_3$ in the cubic phase for simplicity and ease of comparison, the cubic phase of $BaTiO_3$ is known to be stable only at temperatures higher than 120 °C.[31] Because technically, the calculations are performed for the system at low temperature, when the symmetry is broken, despite the constraints of the external structure to be cubic, $BaTiO_3$ gains some energy by internal structure distortions even without any defect. In order to obtain correct hole localization energy, this distorted structure, which is the lowest calculated energy, is used as the reference point for the ground-state energy of pure $BaTiO_3$ (see supplementary material).

III. RESULTS AND DISCUSSION

To simulate a hole in $BaTiO_3$, we removed an electron from the supercell. Removal of an electron from the valence band of the perfect, non-distorted $BaTiO_3$ lattice geometry results in the delocalized hole state, i.e., with a hole at the top of the valence band (valence-band maximum, VBM). The hole state is uniformly distributed over the whole supercell. However, a localized hole can be stabilized by initially extending the Ti-O bonds around one of the oxygen atoms. In the view of the electronic states, the extension of the Ti-O bonds leads to an in-gap state, and the hole is placed in this state instead of the VBM. Figure 1 shows the density of states (DOS) of the $BaTiO_3$ and $SrTiO_3$ supercell containing a localized hole and the charge density associated with the localized hole state in the gap, which is at 1.07 eV above the VBM in $BaTiO_3$. For comparison, the localized hole state at 0.82 eV above the VBM in $SrTiO_3$ is also shown.

The charge density of the hole state (Fig. 1) in both $BaTiO_3$ and $SrTiO_3$ shows a strong O $2p$ orbital character, mostly localized on one O atom, with a very small distribution on the neighboring O atoms. The localization arises from the strong coupling to lattice; the localized charge and the local lattice distortion are the small polaron.[40]

The stability of the STH is determined by the difference between total energies of the localized hole h^+_{polaron} (including the energy cost of the local lattice distortion) and the delocalized hole h^+_{VBM} in the perfect supercell, which we define as the hole self-trapping energy E_{ST}

$$E_{\text{ST}} = E_{\text{tot}}\left[\text{BaTiO}_3 : h^+_{\text{polaron}}\right] - E_{\text{tot}}\left[\text{BaTiO}_3 : h^+_{\text{VBM}}\right], \quad (1)$$

where $E_{\text{tot}}[\text{BaTiO}_3 : h^+_{\text{VBM}}]$ is the total energy of the supercell containing a delocalized hole in the VBM and $E_{\text{tot}}[\text{BaTiO}_3 : h^+_{\text{polaron}}]$ is the total energy of the supercell containing the STH. The calculated E_{ST} is −0.20 eV in $BaTiO_3$, which is much larger in magnitude than in $SrTiO_3$ (−0.04 eV); previous calculations reported values of −0.013 eV (Ref. 28) and −0.05 eV (Ref. 13) for STH in $SrTiO_3$. These negative

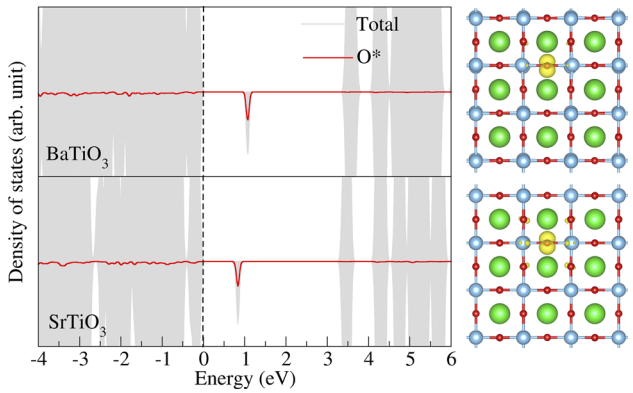

FIG. 1. Calculated density of states (DOS) of $BaTiO_3$ and $SrTiO_3$ containing the self-trapped hole. The dashed vertical line in the DOS plot indicates the highest occupied state. Charge distributions of the polaronic hole state localized on the oxygen atom (O*) are shown on the right.

values of E_{ST} indicate that the hole prefers to be self-trapped instead of delocalized. The larger $|E_{ST}|$ in $BaTiO_3$ than in $SrTiO_3$ indicates a stronger tendency for localization (trapping), which is consistent with the position of the STH state with respect to the VBM (1.07 *vs.* 0.82 eV). Our calculated E_{ST} in $BaTiO_3$ is also in good agreement with the previously calculated value of −0.25 eV by HSE06.[41] The two local Ti-O bonds are elongated by 6.3% in $BaTiO_3$ and by 4.5% in $SrTiO_3$. To understand the large difference in E_{ST} between $BaTiO_3$ and $SrTiO_3$, we decompose self-trapping energy into electronic and strain contributions[25]

$$E_{ST} = E_{LAT} + E_{EL}. \quad (2)$$

We define the strain energy contribution (E_{LAT}) as the energy difference between the supercells with and without the lattice distortion associated with the small polaron but in the charge neutral state. This term represents the energy required to distort the lattice to accommodate the small polaron. The electronic contribution is thus $E_{EL} = E_{ST} - E_{LAT}$, which is related to the position of the hole state with respect to the VBM, i.e., the electronic energy gained by placing the hole in the localized *p*-like state in the gap. We find $E_{LAT} = 0.66$ eV in $BaTiO_3$ and 0.60 eV in $SrTiO_3$ while $E_{EL} = -0.86$ eV in $BaTiO_3$ and −0.64 eV in $SrTiO_3$, as listed in Table I. The STH is more stable in $BaTiO_3$ compared to $SrTiO_3$ due in large part to the electronic energy. The energy penalty to distort the lattice to accommodate the small polaron is comparable in both $BaTiO_3$ and $SrTiO_3$.

We also evaluated the energy barrier between the delocalized hole and the STH configuration by calculating the total energies for a series of intermediate structures, constructed by interpolating the atomic positions between undistorted (delocalized hole) and distorted (self-trapped hole) lattice geometries. In $BaTiO_3$, we find almost no energy barrier as shown in Fig. 2, in contrast to the results reported for the binary oxides.[24] Our result suggests that once a hole is created in the valence band of $BaTiO_3$, it will be readily converted into a self-trapped hole.

In addition, to assure the stability of STH in the room-temperature phase of $BaTiO_3$, we adopted the tetragonal 135-atom supercell to simulate a hole in the valence band. Using similar settings as for cubic $BaTiO_3$, a bandgap (indirect) of 3.04 eV and lattice parameters, $a = 3.968$ Å and $c/a = 1.043$, were obtained. We find that in tetragonal $BaTiO_3$, the hole also prefers self-trapping to delocalization. Due to the symmetry, now there are two possible self-trapped hole configurations: the in-plane and out-of-plane configurations. The self-trapped hole

TABLE I. Self-trapping energy (E_{ST}) of the hole polaron in $BaTiO_3$ and $SrTiO_3$. Lattice strain energy (E_{LAT}) and electronic energy (E_{EL}) are also listed.

	E_{ST} (eV)	E_{LAT} (eV)	E_{EL} (eV)
Cubic $SrTiO_3$	−0.04	0.60	−0.64
Cubic $BaTiO_3$	−0.20	0.66	−0.86
Tetragonal $BaTiO_3$			
Out-of-plane	−0.01	0.90	−0.91
In-plane	−0.22	0.63	−0.85

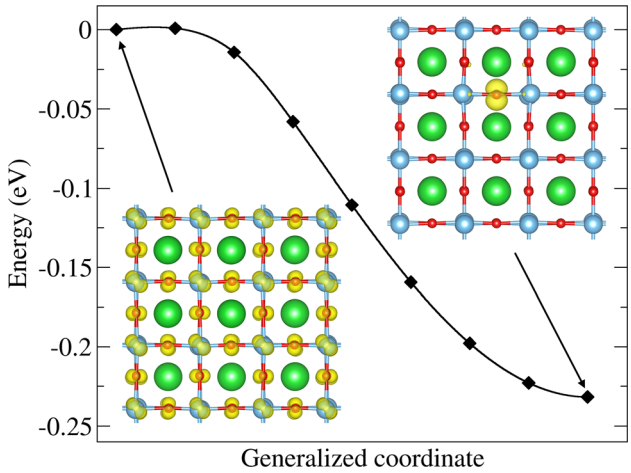

FIG. 2. Configuration coordinate diagram for the transition from the delocalized hole to the localized hole in $BaTiO_3$.

localizing on the in-plane and out-of-plane O atoms (Fig. 3) gives E_{ST} of −0.22 and −0.01 eV, respectively. Much larger value of E_{ST} in the in-plane configuration compared to that the in out-of-plane configuration suggests that holes are readily self-trapped, localizing on O atoms with Ti-O-Ti bonds along in-plane axes in tetragonal $BaTiO_3$. The strain and electronic energy contributions of both STHs in tetragonal $BaTiO_3$ are listed in Table I. Large E_{EL} of both STHs is consistent with the positions of the STH state with respect to the VBM (∼1.1 eV). The larger E_{ST} of in-plane STH results from the smaller E_{LAT}, since E_{EL} of both STHs are comparable.

Next, we discuss the optical transitions associated with the self-trapped hole by constructing a configuration coordinate diagram based on the Franck-Condon principle as shown in Fig. 4(a). The electron-hole pair is created by an incident photon with energy higher than the bandgap. The hole becomes self-trapped, and the conduction-band electron can recombine with the self-trapped hole, thereby, resulting in light emission with energies lower than the bandgap. Here, the electron is assumed to be located at the conduction-band minimum, and the formation of self-trapped exciton (a conduction-band electron bound to a STH via the Coulomb interaction) is neglected. Our calculated emission peak energy in $BaTiO_3$ is 2.17 eV, slightly smaller than the experimentally observed photoluminescence (PL) centered at 2.43 eV at 77 K.[18,19] This discrepancy could be attributed to the difference in the calculated and experimental bandgap of $BaTiO_3$ or to the restriction of Franck-Condon approximation in which the electronic transition must be much faster than the

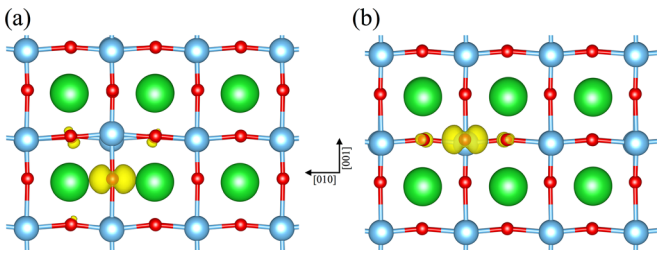

FIG. 3. Charge distributions of the polaronic hole state localized on the (a) out-of-plane and (b) in-plane oxygen atoms.

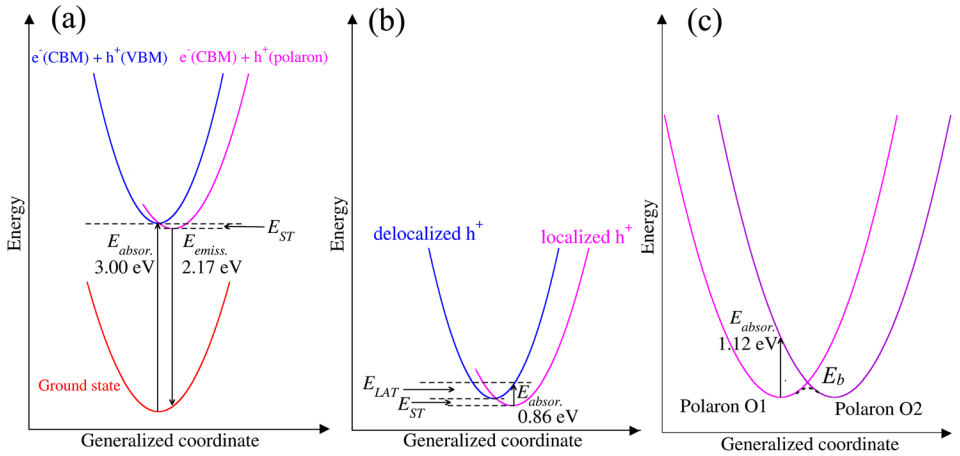

FIG. 4. Schematic diagrams of the optical emission and absorption mechanism of self-trapped holes in $BaTiO_3$. (a) An photoexcited electron in the conduction band recombines with the self-trapped hole, resulting in light luminescence centered at about 2.17 eV, (b) the transition from the localized hole state to the delocalized hole state in the valence band, and (c) the transition between two neighboring polaronic states. E_{absor} is estimated by $4E_b$ as described in the text.

lattice relaxation. Nevertheless, our test calculations give the emission peak associated with STH of ∼2.2 eV, regardless of α values (0.20 and 0.30). The interaction of STH and native defects also could be a source of this discrepancy. A large half-width of 0.9 eV (Ref. 19) suggests that the observed PL peak involves strong electron-phonon coupling, with a large Stokes shift due to the large lattice distortions, as in the case of the STH. Using a similar procedure, we find that both STHs in tetragonal $BaTiO_3$ yield the emission peak energy of 2.25 eV, close to the value obtained in the cubic phase.

The smaller value of calculated emission energy of 2.17 eV in $BaTiO_3$ compared to that in $SrTiO_3$ of 2.47 eV is consistent with the deeper hole-trapped state (Fig. 1) at which photoexcited electrons recombine with self-trapped holes, considering that the bandgaps of $BaTiO_3$ and $SrTiO_3$ are comparable. Since E_{ST} is much larger in $BaTiO_3$ than in $SrTiO_3$, we thus expect that holes can be readily self-trapped in $BaTiO_3$ at higher temperatures much higher than in $SrTiO_3$.

Since small hole polarons introduce unoccupied states in the bandgap, electrons in the valence band can be transferred to the polaronic states by light absorption, leaving delocalized holes in the valence band, as shown in Fig. 4(b). The delocalized holes subsequently become self-trapped again by emitting or absorbing phonons. The absorption energy is given by the energy difference between the supercell containing the delocalized hole state but in the STH lattice configuration and the supercell containing STH in its relaxed lattice configuration. However, the total energy of the supercell containing the delocalized hole in the STH lattice configuration is inaccessible. The absorption peak is thus estimated by the sum of the modulus of E_{ST} (0.20 eV) and E_{LAT} (0.66 eV), which is 0.86 eV.

We also considered another optical excitation mechanism involving a hopping process. In this mechanism, the small polaron is excited out of its self-trapping potential well and is subsequently transferred to another self-trapping state accompanied by a lattice distortion at a neighboring lattice site. This transition between two localized states corresponds to the photon-assisted hopping of the polarons, as shown in Fig. 4(c). The absorption energy is given by the energy difference between the initial state in which the hole is localized on a given O atom (O1) and a final state in which the hole is localized on a neighboring O atom (O2) but with the same lattice configuration as that of the hole localized on the O atom in the initial state. The absorption energy can be estimated from the migration barrier of the polaron as $4E_b = 4 \times 0.28 = 1.12$ eV,[42] where E_b is the migration barrier of the STH, as discussed below.

We address the transport properties associated with the STH by investigating its migration in the $BaTiO_3$ lattice. The mobility of STH can be described by the migration barrier of the STH between two neighboring oxygen sites. To determine this energy barrier, we first performed two separate calculations, one for the small polaron on the O1 and the other on the O2 atoms. An interpolation scheme was used to determine the intermediate configurations for which the atomic positions are $\mathbf{R} = x\mathbf{R}_i + (1-x)\mathbf{R}_f$, where $\mathbf{R}_i$ and $\mathbf{R}_f$ are the coordinates of all atoms in the supercell associated with initial and final configurations. The electronic structure for each intermediate configuration was then solved self-consistently, and the total-energy difference between intermediate configurations and initial and final configuration is plotted in Fig. 5(a). The saddle point $x = 0.5$ in the migration path yields an energy barrier of 0.28 eV. The higher energy barrier in $BaTiO_3$ compared to $SrTiO_3$ ($E_b = 0.07$ eV)[28] is consistent with the more localized hole state in $BaTiO_3$. In addition, we analyzed the Bader charge[43] on the two neighboring O atoms associated with the small polaron hopping. The maximum absence of electrons of $+0.34e$ with respect to an O atom without STH is actually found on the O1 and O2 atoms for $x = 0$ and 1, respectively. Figure 5(b) shows the absence of electrons on the two adjacent O atoms as the localized hole migrates from one O atom to the other. At the saddle point, the spin density is equally distributed on the two neighboring O atoms (electron absence of $+0.12e$ each). The corresponding atomic configurations and the spin density of the small polaron in the migration path, shown in Fig. 5(c), reveal that the STH is gradually transferred from one O site to the nearest neighbor O as x increases.

If the migration of small polarons occurs through thermally activated hopping, the hole mobility (μ) can be approximated by $\mu = [ea^2\omega_0/k_BT][\exp(-E_b/k_BT)]$, where a is the hopping distance, i.e., the distance between the neighboring oxygen atoms, ω_0 is the longitudinal phonon frequency, and E_b is the energy barrier for polaron hopping displayed in Fig. 5(a). Using $E_b = 0.28$ eV from our calculations, $a = 2.819$ Å

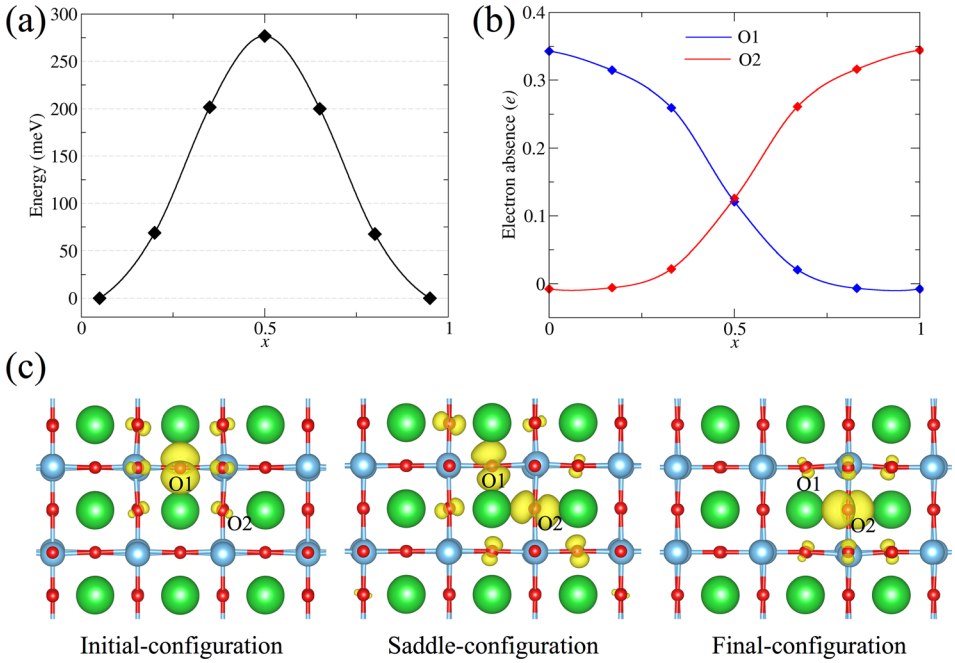

FIG. 5. (a) Migration energy barrier for a small hole-polaron in $BaTiO_3$. (b) The absence of the electron on the neighboring O atoms associated with a small hole-polaron migration using the Bader charge analysis. (c) The corresponding charge distribution for the polaron migration at the initial, saddle-point, and final configurations.

and $\omega_0 = 700\,\mathrm{cm}^{-1}$,[44] the hole mobility at room temperature (300 K) in $BaTiO_3$ is 1.28×10^{-5} cm^2 V^{-1} s^{-1}. This low value of hole mobility indicates that any holes introduced in $BaTiO_3$, by, e.g., doping with shallow acceptors, will be all self-trapped, and no significant *p*-type conductivity can be obtained. Our calculated energy barrier and hole mobility are in reasonable agreement with the small polaron activation energy of 0.15 ± 0.4 eV and mobility of $(3 \pm 1) \times 10^{-3}$ cm^2 V^{-1} s^{-1} determined from the drift mobility measurements at room temperature, which performed on well-insulating $BaTiO_3$ single crystals.[21] [Note that the mobility is sensitive to the energy barrier since it exponentially depends on the barrier height. Thus, the discrepancy found in the experimental and theoretical values of mobility is considered to be due to the slight overestimation of E_b. The estimation can be improved by using more accurate computational method such as the nudge elastic band (NEB), which is likely to yield a smaller value of E_b and should result in a higher mobility.] Our calculated STH and its migration barrier suggest that it could be responsible for the transport properties observed by Boyeaux and Michel-Calendini.[21] Although, in their original work, Boyeaux and Michel-Calendini assigned the observed properties to electron small polaron, we believe that electron small polaron and hole polaron can equally be the candidate for the observed properties, and they even could coexist. The actual dominant mechanism is still unclear. Computational investigation to determine the stability of electron polaron is underway. Additional experiments are encouraged to provide more detailed investigation of the optical and transport properties of the small polarons in $BaTiO_3$ as advanced probing methods and high-quality crystals are available nowadays.

IV. CONCLUSION

We have investigated the small hole polaron in cubic $BaTiO_3$ using hybrid density-functional calculations. We find that the hole in the valence band favors localization on one of the oxygen atoms, accompanied by a local lattice distortion. The large self-trapping energy indicates that the hole polaron in $BaTiO_3$ should be stable up to room temperature and, thus, are likely to contribute to the experimental observations. Our calculations show that the self-trapped hole gives rise to the optical emission peak at about 2.17 eV, in reasonable agreement with the experimentally observed photoluminescence. We also provide optical-absorption values associated with the hole polaron that should guide the future experiments. The calculated migration barrier of the polaron indicates a very low mobility of the hole polaron, suggesting that no significant *p*-type conductivity can be obtained in $BaTiO_3$. Our calculated migration barrier and mobility of the hole polaron are in reasonable agreement with available experimental values.

SUPPLEMENTARY MATERIAL

See supplementary material for details of distorted cubic supercell and self-interaction error.

ACKNOWLEDGMENTS

This work was supported by the Thailand Research Funds (Contract No. TRG5780260) and Institute for Promotion of Science and Technology (DPST Research Grant No. 036/2557). P.R. and J.T. acknowledge Kasetsart University Research and Development Institute (KURDI). A.J. was supported by the National Science Foundation under Grant No. DMR-1652994. We wish to thank the High-Performance Computing Center at Synchrotron Light Research Institute (SLRI, Thailand) for their hospitality.

[1]M. N. Kamalasanan, S. Chandra, P. C. Joshi, and A. Mansingh, Appl. Phys. Lett. **59**(27), 3547–3549 (1991).
[2]Z.-X. Chen, Y. Chen, and Y.-S. Jiang, J. Phys. Chem. B **105**(24), 5766–5771 (2001).

[3]K. J. Choi, M. Biegalski, Y. L. Li, A. Sharan, J. Schubert, R. Uecker, P. Reiche, Y. B. Chen, X. Q. Pan, V. Gopalan, L.-Q. Chen, D. G. Schlom, and C. B. Eom, Science **306**(5698), 1005–1009 (2004).
[4]M. T. Buscaglia, M. Viviani, V. Buscaglia, L. Mitoseriu, A. Testino, P. Nanni, Z. Zhao, M. Nygren, C. Harnagea, D. Piazza, and C. Galassi, Phys. Rev. B **73**(6), 064114 (2006).
[5]H. Kumazawa and K. Masuda, Thin Solid Films **353**(1), 144–148 (1999).
[6]D. Kip, Appl. Phys. B **67**(2), 131–150 (1998).
[7]K. Hiroshi, M. Youichi, and C. Hirokazu, Jpn. J. Appl. Phys., Part 1 **42**(1R), 1 (2003).
[8]J. Y. Lee, J. H. Lee, S. H. Hong, Y. K. Lee, and J. Y. Choi, Adv. Mater. **15**(19), 1655–1658 (2003).
[9]F. A. Yildirim, C. Ucurum, R. R. Schliewe, W. Bauhofer, R. M. Meixner, H. Goebel, and W. Krautschneider, Appl. Phys. Lett. **90**(8), 083501 (2007).
[10]Y. Cui, J. Briscoe, and S. Dunn, Chem. Mater. **25**(21), 4215–4223 (2013).
[11]H. Fan, H. Li, B. Liu, Y. Lu, T. Xie, and D. Wang, ACS Appl. Mater. Interfaces **4**(9), 4853–4857 (2012).
[12]E. Krätzig, F. Welz, R. Orlowski, V. Doormann, and M. Rosenkranz, Solid State Commun. **34**(10), 817–819 (1980).
[13]A. Janotti, J. B. Varley, M. Choi, and C. G. Van de Walle, Phys. Rev. B **90**(8), 085202 (2014).
[14]V. M. Fridkin and B. N. Popov, Ferroelectrics **21**(1), 611–613 (1978).
[15]S. Ducharme and J. Feinberg, J. Appl. Phys. **56**(3), 839–842 (1984).
[16]D. Mahgerefteh and J. Feinberg, Phys. Rev. Lett. **64**(18), 2195–2198 (1990).
[17]D. Mahgerefteh and J. Feinberg, Mod. Phys. Lett. B **05**(10), 693–700 (1991).
[18]M. Aguilar, C. Gonzalo, and G. Godefroy, Ferroelectrics **25**(1), 467–470 (1980).
[19]M. Aguilar, C. Gonzalo, and G. Godefroy, Solid State Commun. **30**(8), 525–529 (1979).
[20]H. Ihrig, J. H. T. Hengst, and M. Klerk, Z. Phys. B **40**(4), 301–306 (1981).
[21]J. P. Boyeaux and F. M. Michel-Calendini, J. Phys. C **12**(3), 545 (1979).
[22]A. Stashans and H. Pinto, Int. J. Quantum Chem. **79**(6), 358–366 (2000).
[23]R. I. Eglitis, E. A. Kotomin, and G. Borstel, Eur. Phys. J. B **27**(4), 483–486 (2002).
[24]J. B. Varley, A. Janotti, C. Franchini, and C. G. Van de Walle, Phys. Rev. B **85**(8), 081109 (2012).
[25]L. Sun, X. Huang, L. Wang, and A. Janotti, Phys. Rev. B **95**(24), 245101 (2017).
[26]B. J. Morgan and G. W. Watson, Phys. Rev. B **80**(23), 233102 (2009).
[27]L. Bjaalie, D. G. Ouellette, P. Moetakef, T. A. Cain, A. Janotti, B. Himmetoglu, S. J. Allen, S. Stemmer, and C. G V d Walle, Appl. Phys. Lett. **106**(23), 232103 (2015).
[28]H. Chen and N. Umezawa, Phys. Rev. B **90**(3), 035202 (2014).
[29]J. Heyd, G. Scuseria, and M. Ernzerhof, J. Chem. Phys. **118**(18), 8207–8215 (2003).
[30]G. Kresse and J. Furthmüller, Phys. Rev. B **54**(16), 11169–11186 (1996).
[31]S. H. Wemple, Phys. Rev. B **2**(7), 2679–2689 (1970).
[32]S. Miyake and R. Ueda, J. Phys. Soc. Jpn. **2**(5), 93–97 (1947).
[33]G. Pacchioni, F. Frigoli, D. Ricci, and J. A. Weil, Phys. Rev. B **63**(5), 054102 (2000).
[34]D. O. Scanlon, A. Walsh, B. J. Morgan, M. Nolan, J. Fearon, and G. W. Watson, J. Phys. Chem. C **111**(22), 7971–7979 (2007).
[35]M. d'Avezac, M. Calandra, and F. Mauri, Phys. Rev. B **71**(20), 205210 (2005).
[36]P. Deák, B. Aradi, T. Frauenheim, E. Janzén, and A. Gali, Phys. Rev. B **81**(15), 153203 (2010).
[37]P. Deák, B. Aradi, and T. Frauenheim, Phys. Rev. B **83**(15), 155207 (2011).
[38]Y. K. Frodason, K. M. Johansen, T. S. Bjørheim, B. G. Svensson, and A. Alkauskas, Phys. Rev. B **95**(9), 094105 (2017).
[39]P. Deák, Q. Duy Ho, F. Seemann, B. Aradi, M. Lorke, and T. Frauenheim, Phys. Rev. B **95**(7), 075208 (2017).
[40]A. L. Shluger and A. M. Stoneham, J. Phys. Condens. Matter **5**(19), 3049 (1993).
[41]P. Erhart, A. Klein, D. Åberg, and B. Sadigh, Phys. Rev. B **90**(3), 035204 (2014).
[42]I. G. Austin and N. F. Mott, Adv. Phys. **50**(7), 757–812 (2001).
[43]G. Henkelman, A. Arnaldsson, and H. Jónsson, Comput. Mater. Sci. **36**(3), 354–360 (2006).
[44]W. Zhong, R. D. King-Smith, and D. Vanderbilt, Phys. Rev. Lett. **72**(22), 3618–3621 (1994).